3-2005

Acoustic Radiation Modes of a Tire on a Reflecting Surface

Kiho Yum
Purdue University

Kwanwoo Hong
Purdue University

J Stuart Bolton
Purdue University, bolton@purdue.edu

Acoustic Radiation Modes of a Tire on a Reflecting Surface

Kiho Yum, Kwanwoo Hong and J. Stuart Bolton

Ray W. Herrick Laboratories

Purdue University

West Lafayette, Indiana, USA

LMS User Conference 2005

Troy, Michigan, USA

March 15 -16, 2005

PURDUE UNIVERSITY

HERRICK LABORATORIES

Radiation Mode Approach

- **Radiation Mode Approach is used in**
  - Active noise control
  - Source reconstruction
  - Acoustic design optimization

- **Objectives**
  - To implement a radiation mode approach to tire noise radiation by using SYSNOISE ATV function
  - To identify tire noise generation mechanism

- **Problem Definition**
  - Acoustic radiation modes of a rectangular plate
  - 3-dimensional radiation field characteristics resulting from the tire and ground geometry

Acoustic Radiation Modes

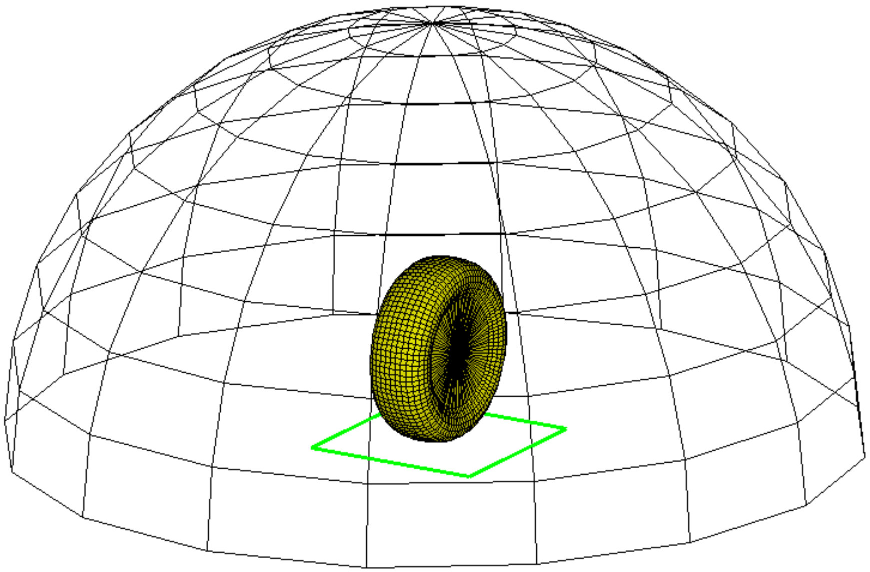

- defined on the surface of the structure.
- shows the orthogonal characteristics of the radiation field surrounding the structure.
- acoustic radiation mode identifies the effective radiation region on the structure surface.
- dependent on geometry of the structure, not on surface velocity distribution of the structure.

Acoustic Transfer Vector (ATV)

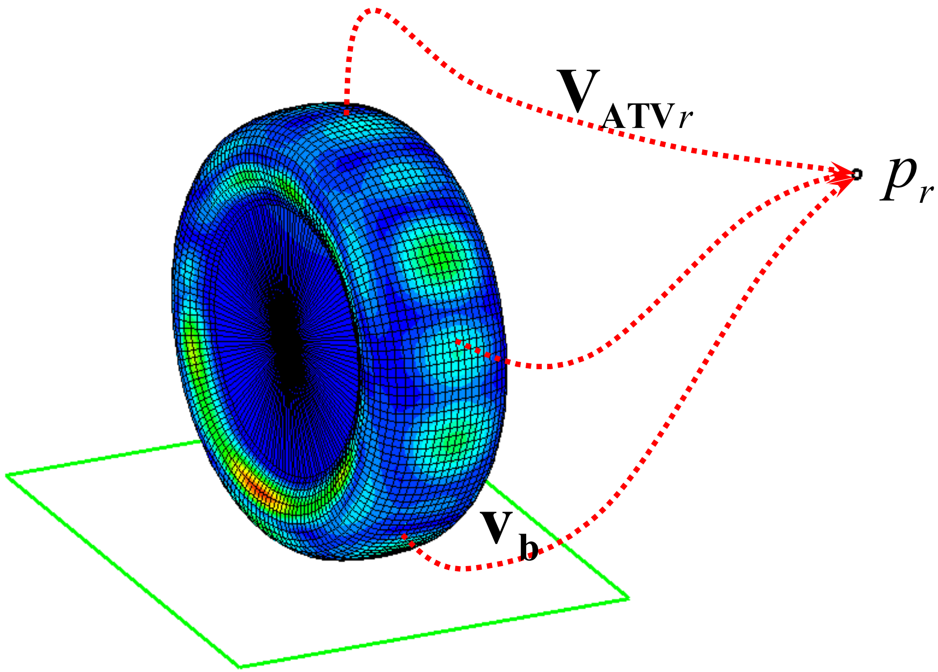

$$p_r = \mathbf{V}_{\mathbf{ATV}r}^{\mathbf{T}} \mathbf{v}_\mathbf{b}$$

b: boundary surface
r: at one field point

- provides base for calculation of the radiation field characteristics.
- relationship between surface normal velocities ($\mathbf{v}_\mathbf{b}$) and radiated sound pressure (p_r) in frequency domain.
- dependent on geometry of vibrating surface, field point location and physical properties of acoustic medium.

Acoustic Transfer Vector (ATV)

Radiation field representation

- Helmholtz integral equation

$$p(\vec{x})\alpha(\vec{x}) = \int_S p(\vec{y})\frac{\partial G(\vec{x}|\vec{y})}{\partial n_y} dS_y + j\rho_0\omega\int_S v(\vec{y})G(\vec{x}|\vec{y})dS_y$$

- Rayleigh integral equation (baffled plate case)

$$p(\vec{x})\alpha(\vec{x}) = j2\rho_0\omega\int_S v(\vec{y})G(\vec{x}|\vec{y})dS_y$$

Discretization

- On the surface: $\mathbf{A}\mathbf{p}_b = \mathbf{B}\mathbf{v}_b$
- In far-field: $p_r = \mathbf{d}^{\mathrm{T}}\mathbf{p}_b + \mathbf{m}^{\mathrm{T}}\mathbf{v}_b$

pressure at a field point (p_r)

pressure & normal velocity on the boundary ($\mathbf{p}_b$, $\mathbf{v}_b$)

$$\mathbf{V}_{\mathrm{ATV}r}^{\mathrm{T}} = \mathbf{d}^{\mathrm{T}}\mathbf{A}^{-1}\mathbf{B} + \mathbf{m}^{\mathrm{T}}$$

ATV

$$p_r = \mathbf{V}_{\mathrm{ATV}r}^{\mathrm{T}}\mathbf{v}_{\mathrm{b}}$$

$$\mathbf{p} = \mathbf{V}_{\mathrm{ATV}}^{\mathrm{T}}\mathbf{v}_{\mathrm{b}}$$

pressure matrix at all field points on the recovery surface ($\mathbf{p}$)

Acoustic Transfer Matrix (ATM) ($\mathbf{V}_{\mathrm{ATV}}^{\mathrm{T}}$)

Sound Radiation Mode

- **Radiated sound power in far-field**

$$W = \sum_{r=1}^{R} \frac{|p_r|^2}{2\rho_0 c} S_r = \sum_{r=1}^{R} \frac{p_r^* p_r}{2\rho_0 c} S_r \quad \xrightarrow[\text{ATV relationship}]{\text{apply}} \quad W = \sum_{r=1}^{R} \frac{\mathbf{v}_b^{\mathbf{H}} \mathbf{V}_{\mathrm{ATV}r}^{*} \mathbf{V}_{\mathrm{ATV}r}^{\mathbf{T}} \mathbf{v}_b}{2\rho_0 c} S_r = \mathbf{v}_b^{\mathbf{H}} \mathbf{R} \mathbf{v}_b$$

▶ $$\mathbf{R} = \sum_{r=1}^{R} \frac{\mathbf{V}_{\mathrm{ATV}r}^{*} \mathbf{V}_{\mathrm{ATV}r}^{\mathbf{T}}}{2\rho_0 c} S_r$$: **Radiation Resistance Matrix**

- **Sound Radiation Mode**: resulting from eigenvector decomposition of radiation resistance matrix

$$\mathbf{R} = \mathbf{Q} \boldsymbol{\Lambda} \mathbf{Q}^{\mathbf{H}}$$

▶ normalized eigenvector $\mathbf{Q}^{\mathbf{H}}$: **Sound Radiation Mode**

▶ eigenvalue $\boldsymbol{\Lambda}$: proportional to radiation efficiency

Plate Radiation Model

■ Baffled Plate Radiation Model

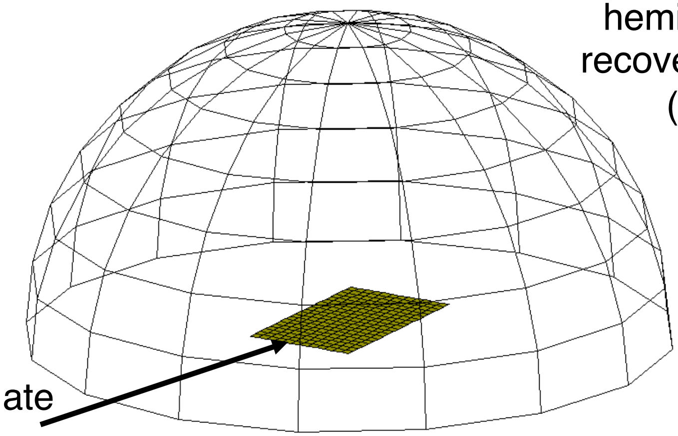

■ ATV Calculation Approach

- Theoretical approach using Rayleigh Theory

$$p(\vec{x}) = \frac{j\omega\rho_0}{2\pi} e^{j\omega t} \int_S \frac{v_n(\vec{y})\, e^{-jkr(\vec{y},\vec{x})}}{r(\vec{y},\vec{x})} dS$$

- Simulation using SYSNOISE (Ver. 5.6) Rayleigh Option

Sound Radiation Modes (320 Hz)

[theory based] [simulation based]

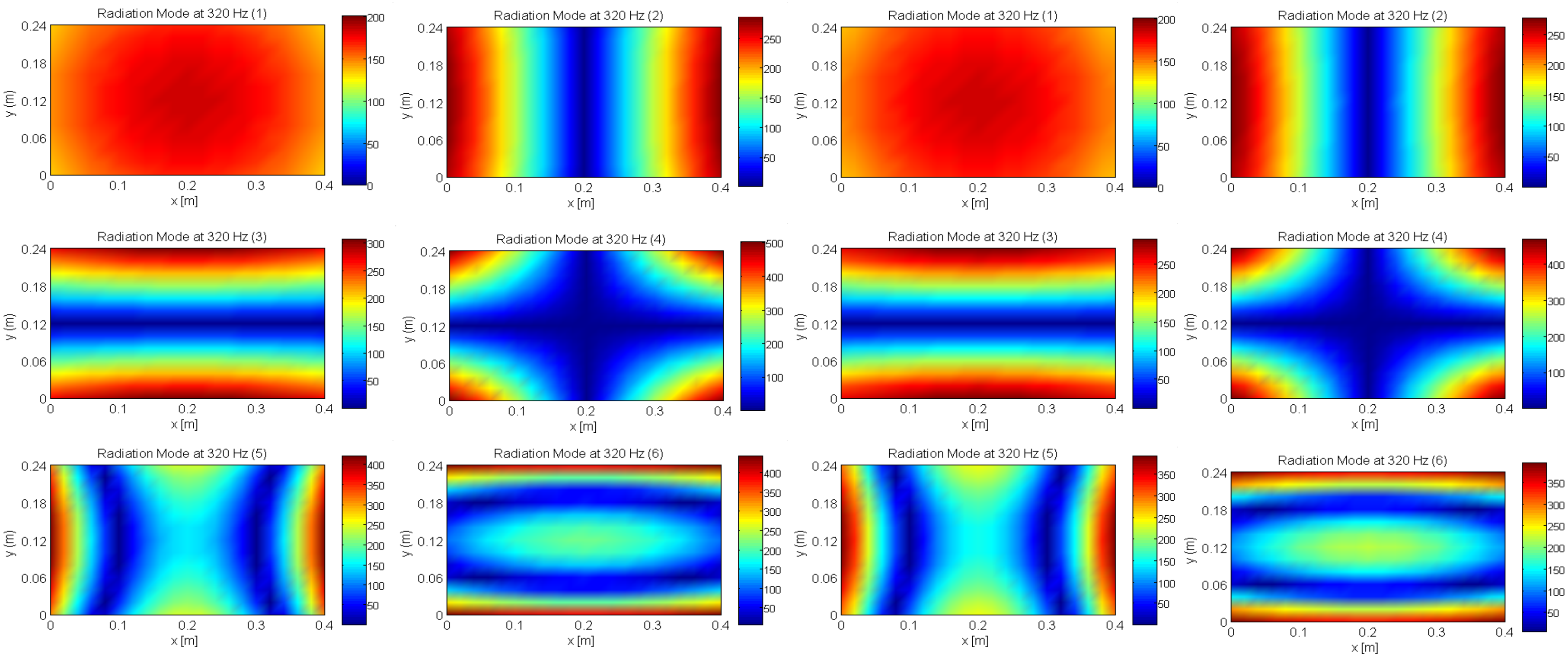

- Amplitude visualization
- Good match between theory and simulation
- Breathing mode is dominant

PURDUE UNIVERSITY

HERRICK LABORATORIES

Sound Radiation Modes (960 Hz)

[theory based] [simulation based]

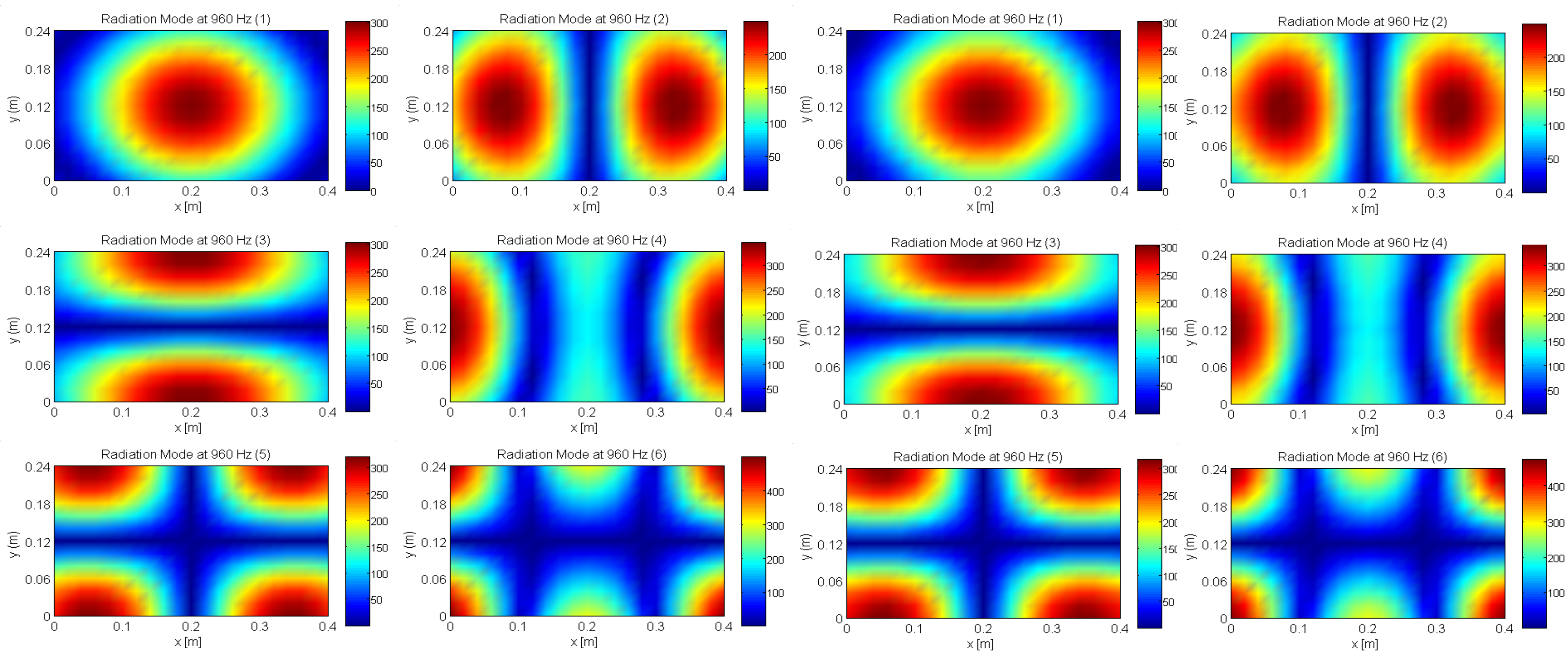

- Good match between theory and simulation
- Radiation from central region stronger than that from the edge.

Eigenvalue of Radiation Modes

■ Eigenvalue of each radiation mode

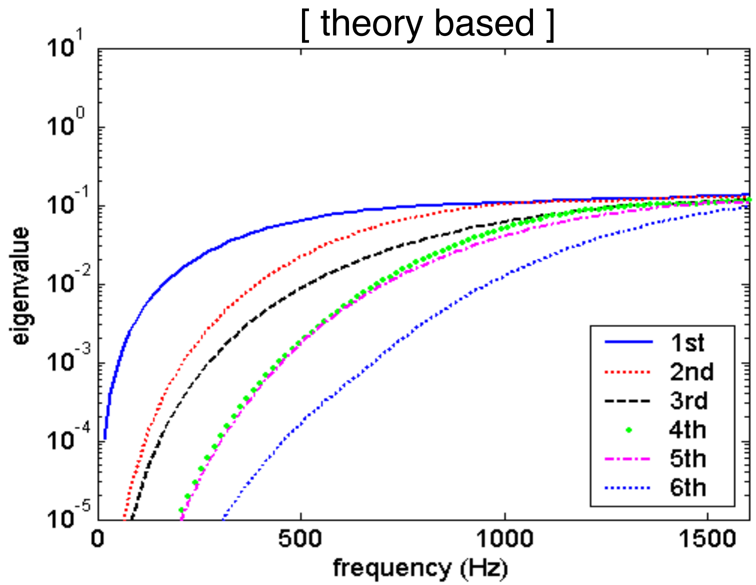

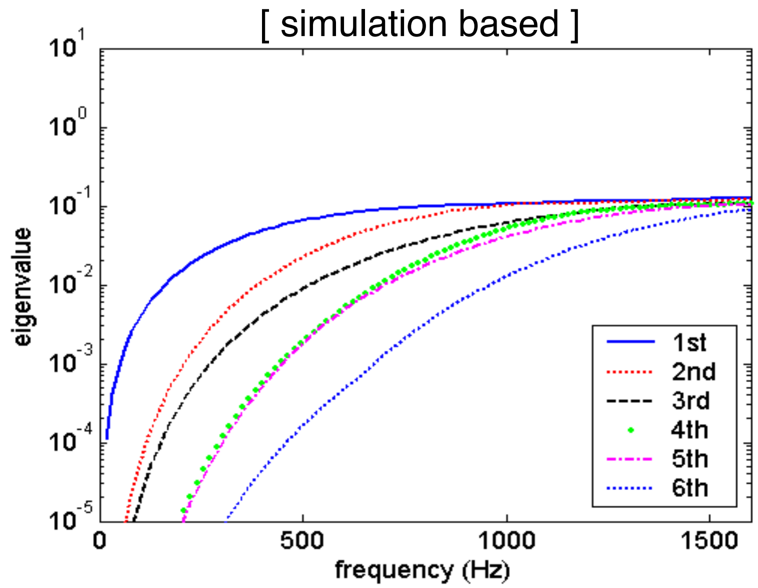

- Good match between theory and simulation.
- As frequency increases, eigenvalue of each radiation mode increases. Eigenvalue stops increasing and converges at the coincidence frequency.
- Eigenvalues are proportional to radiation efficiencies of radiation resistance matrix.

Tire Radiation Analysis Procedure

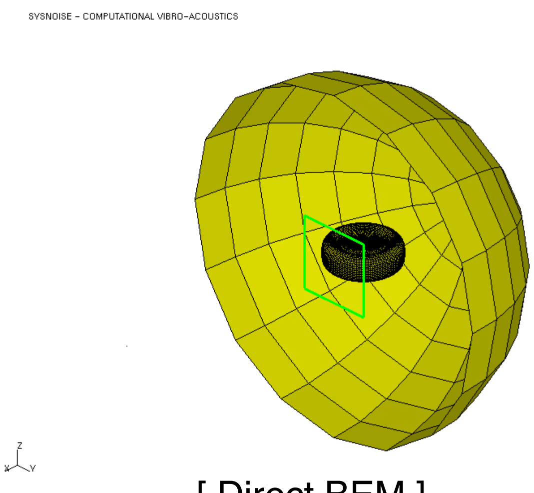

[Direct BEM]

radiation field characteristics
based on Acoustic Radiation Mode
(Acoustic Transfer Vector)

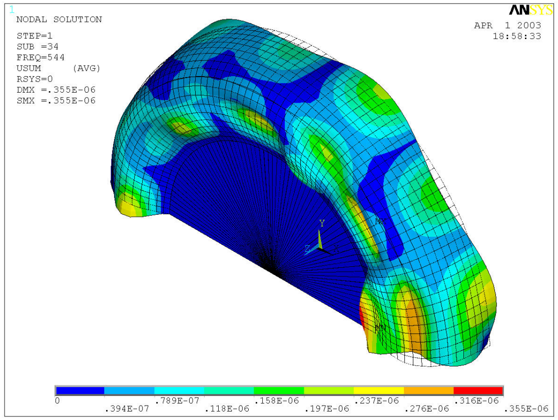

[Structural Harmonic FEM]
structural wave propagation
based on surface normal velocities

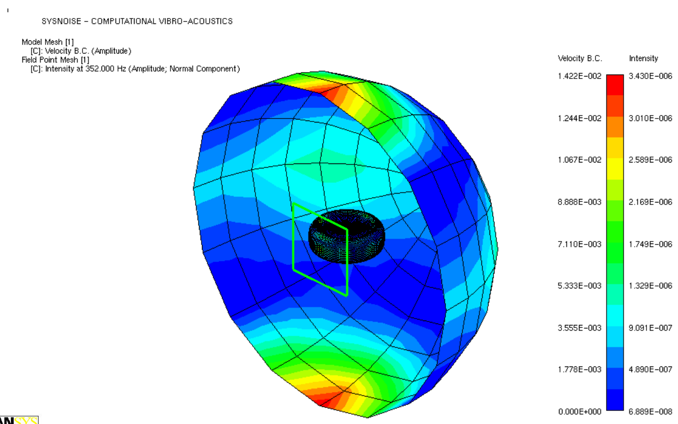

SPL & Sound Intensity
on a hemisphere
surrounding a tire

↓

Sound Power
Radiation Efficiency
Radiation Mode Contribution

PURDUE UNIVERSITY

HERRICK LABORATORIES

Tire Radiation Model

■ Boundary Element Model

- 205/70R14 tire base
- Two radiation cases: free space radiation / reflecting surface radiation
- Recovery surface: R7.5 sphere (hemisphere) – related to pass-by noise test
- For reflecting surface radiation case, the reflecting surface was modeled as rigid.

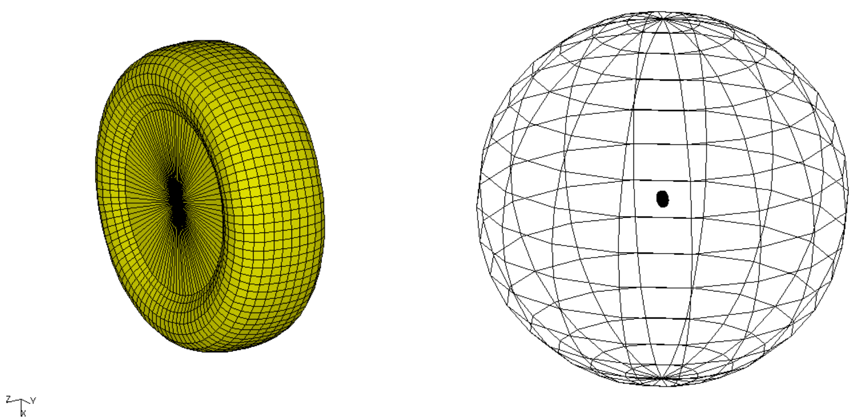

[free space radiation]

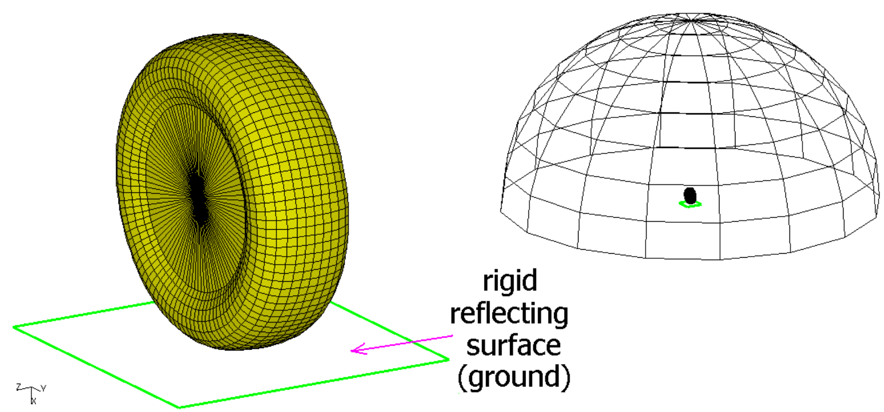

[reflecting surface radiation]

Radiation BE Analysis

■ D-BEM Analysis

- Using Direct Collocation Boundary Element Method (D-BEM) in SYSNOISE ver. 5.6
- Reason to use D-BEM: D-BEM takes less calculation time and allows model simplification for the interior singularity problem
- Frequency range: 12.5 Hz – 1600 Hz (constant bandwidth 12.5 Hz)

■ CHIEF Method

- To eliminate the singularity effect in an exterior D-BEM problem, CHIEF points were introduced inside the tire model.
- The Number and location of CHIEF points were optimized. Finally 18 CHIEF points were applied.

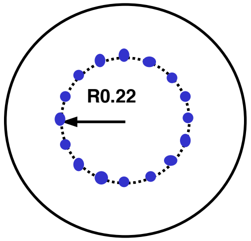

Sound Radiation Modes (350 Hz)

[free space radiation]

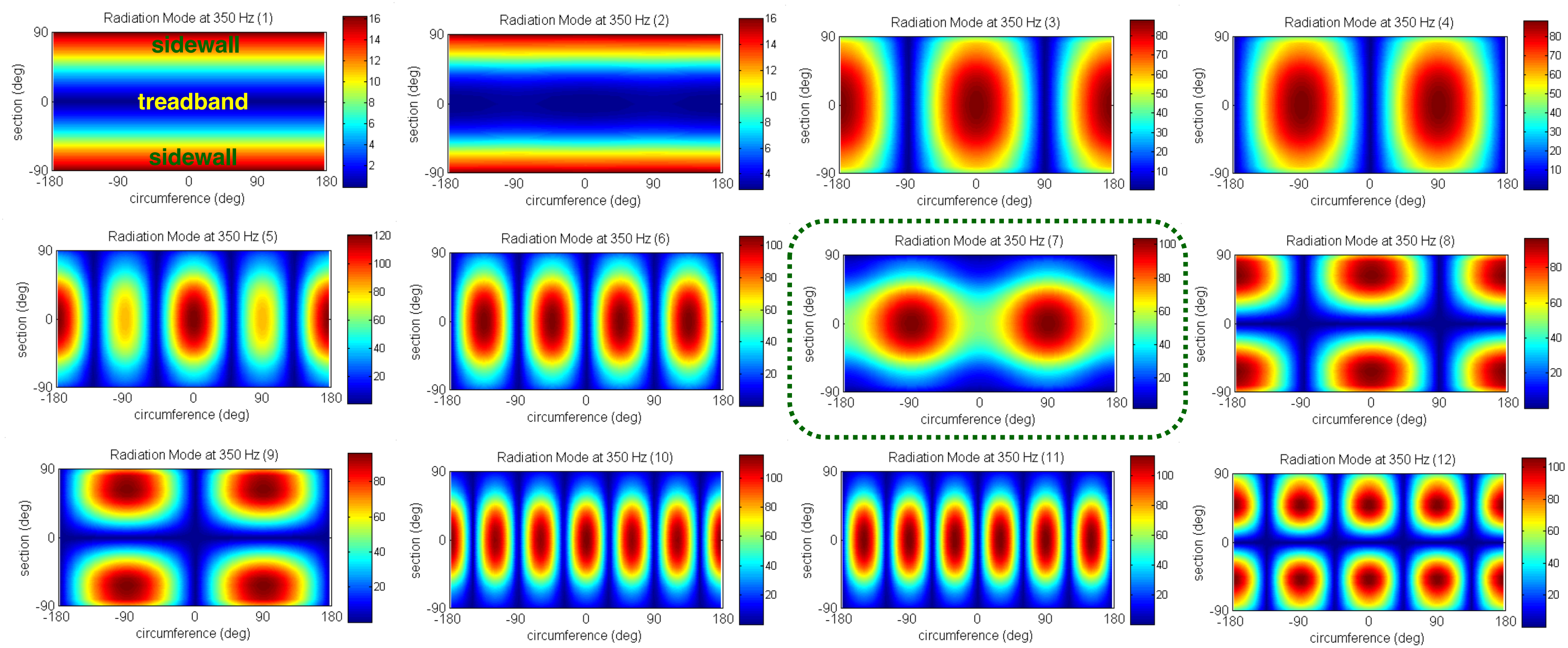

- first and second modes: sidewall and wheel dominant
- grouping characteristics: 3rd and 4th, 5th and 6th, 8th and 9th, 10th and 11th
- 7th mode: ring like mode

Sound Radiation Modes (350 Hz)

[reflecting surface radiation]

point in contact with reflecting surface

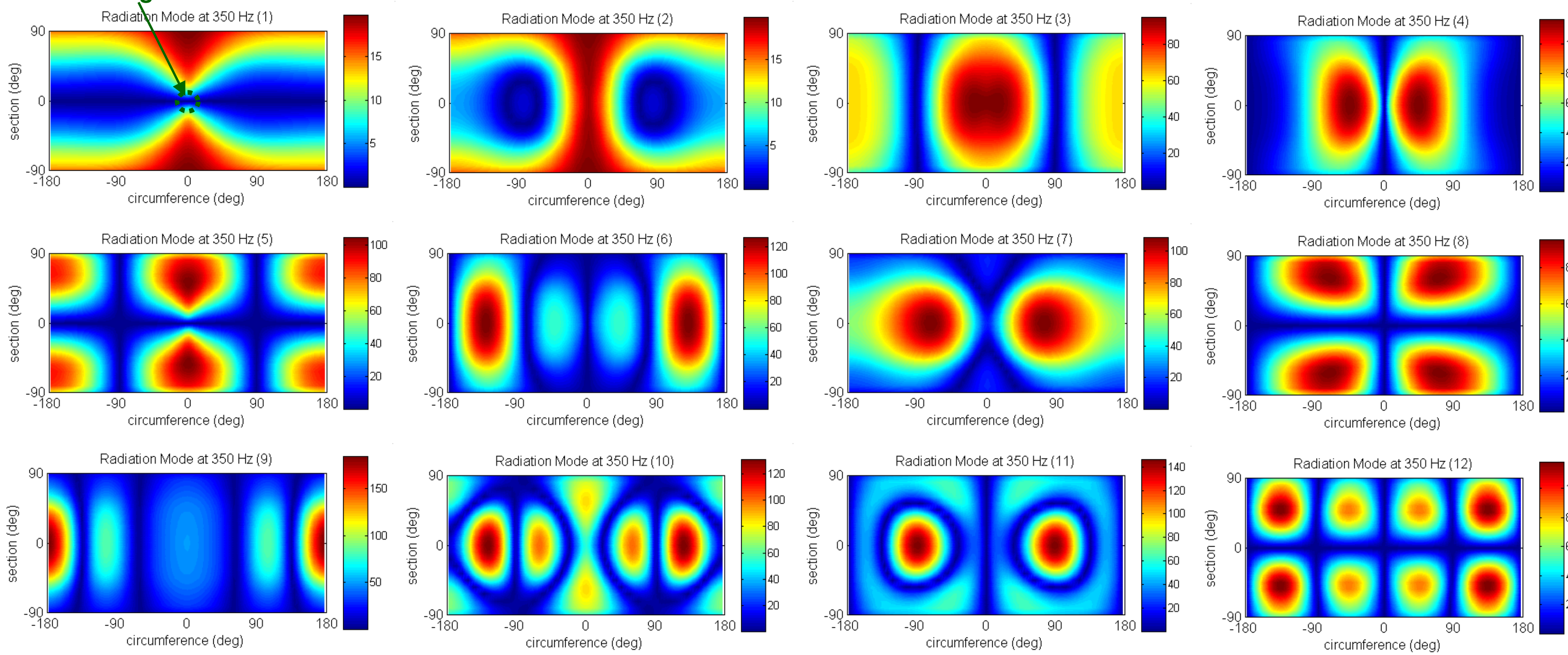

- first and second mode: similar to free space radiation case but a peak is added in the contact patch area
- No grouping characteristic.

Sound Radiation Modes (638 Hz)

[free space radiation]

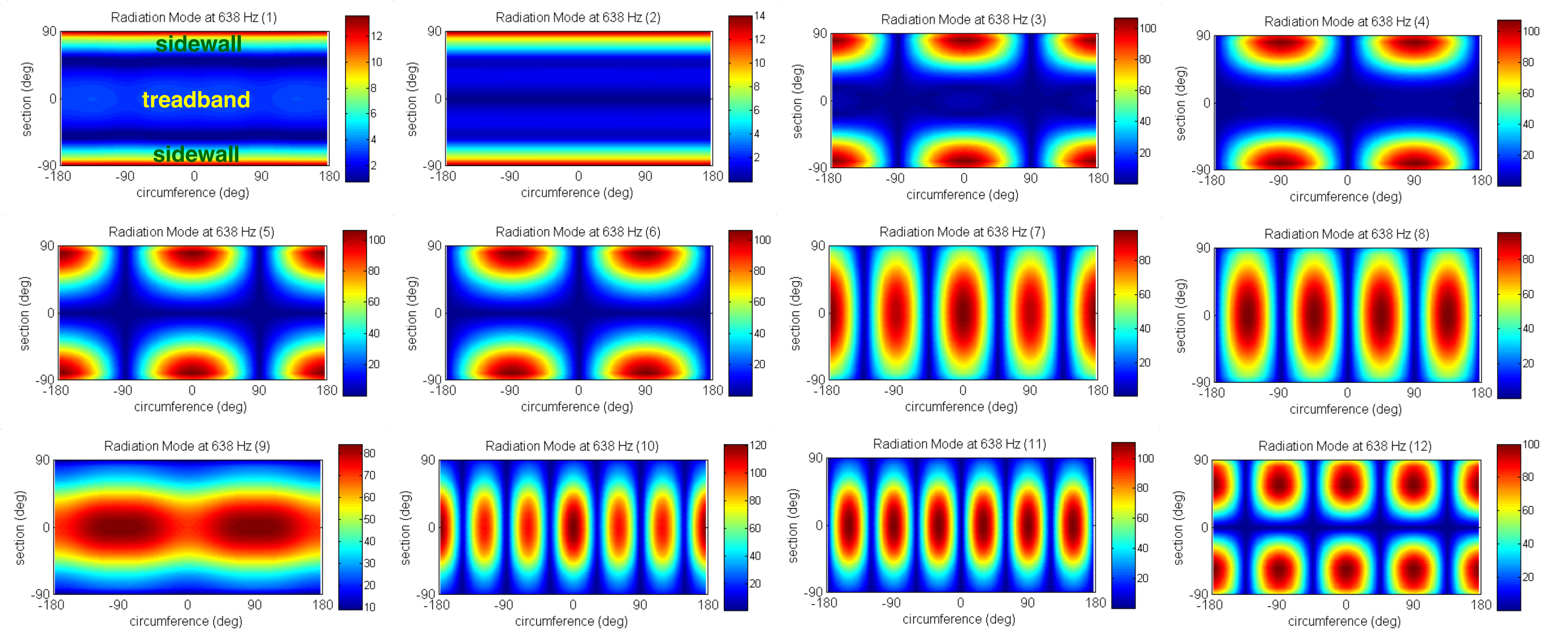

- first and second modes: sidewall and wheel dominant
- grouping characteristics
- oscillating modes which have higher value on the sidewall appear in the lower modes.

PURDUE UNIVERSITY

HERRICK LABORATORIES

Sound Radiation Modes (638 Hz)

[reflecting surface radiation]

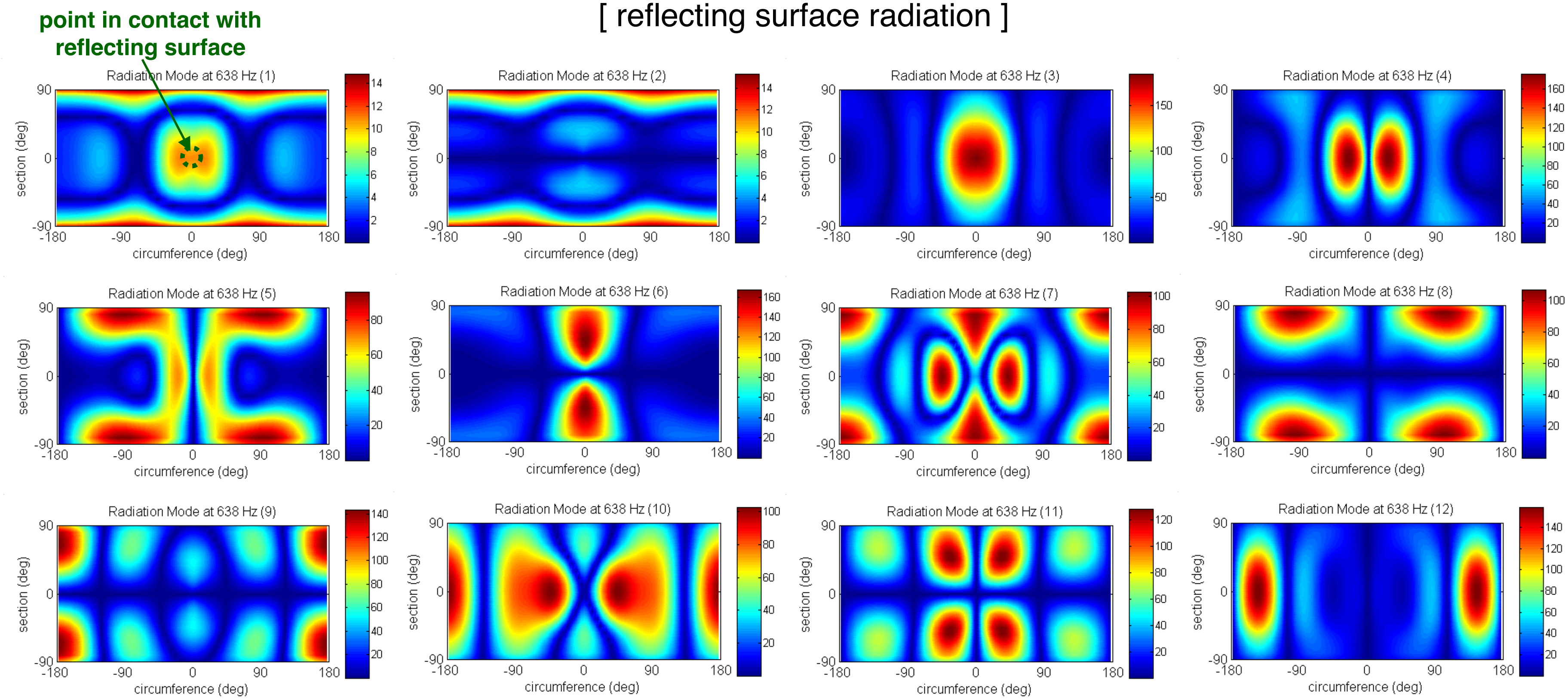

- first and second mode: similar to free space radiation case but a peak is added in the contact patch area
- No grouping characteristic

Sound Radiation Modes (950 Hz)

[free space radiation]

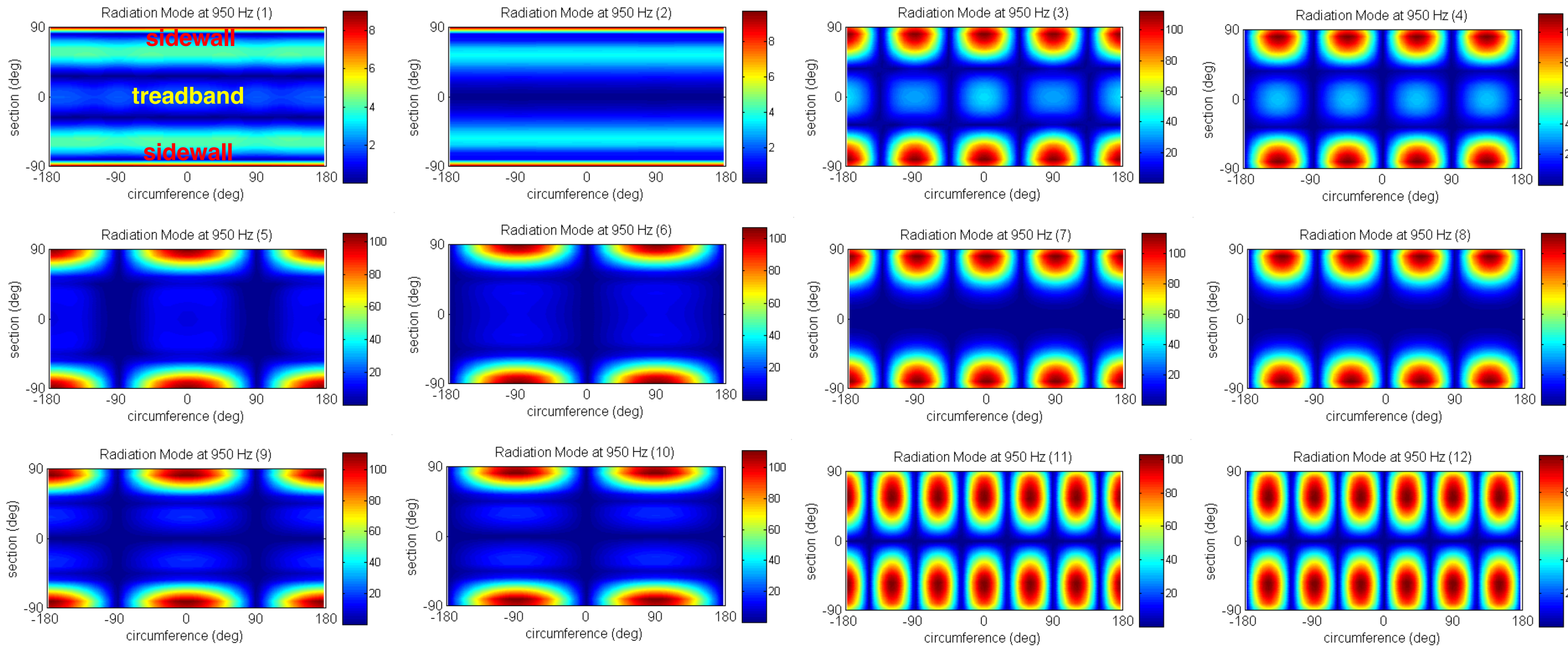

- first mode: wheel dominant
- oscillating modes which have higher value on the sidewall appear in the lower modes.
- treadband is not efficient radiation region

Sound Radiation Modes (950 Hz)

[reflecting surface radiation]

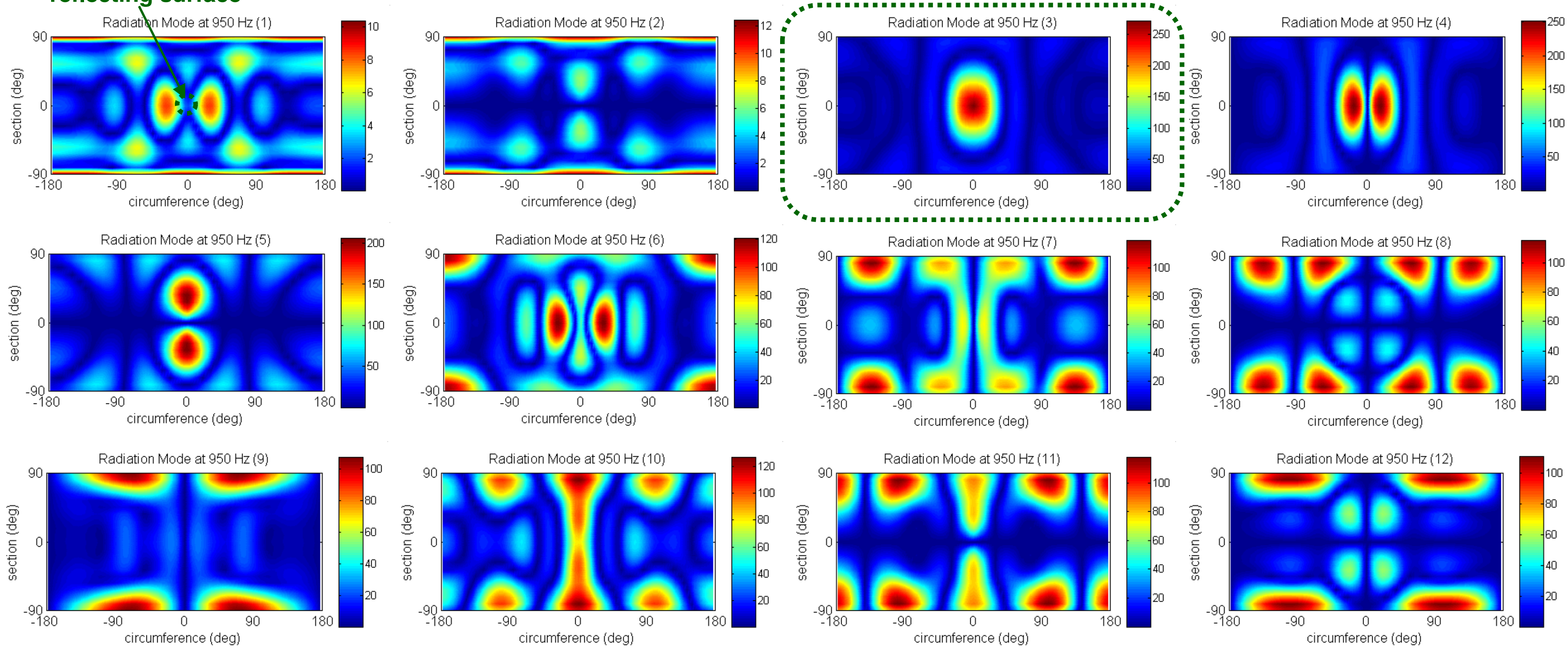

- similar to free space radiation case but a peak is added in the contact patch area.
- 3rd – 5th modes: high radiation region on contact patch area

Radiation Efficiency of Radiation Modes

[free space radiation]

■ Radiation efficiency of each radiation mode for a unit surface normal velocity

$$: \sigma_n = \frac{W}{E} = \frac{2\lambda_n}{\rho_0 c S_b}$$ proportional to eigenvalue of radiation resistance matrix

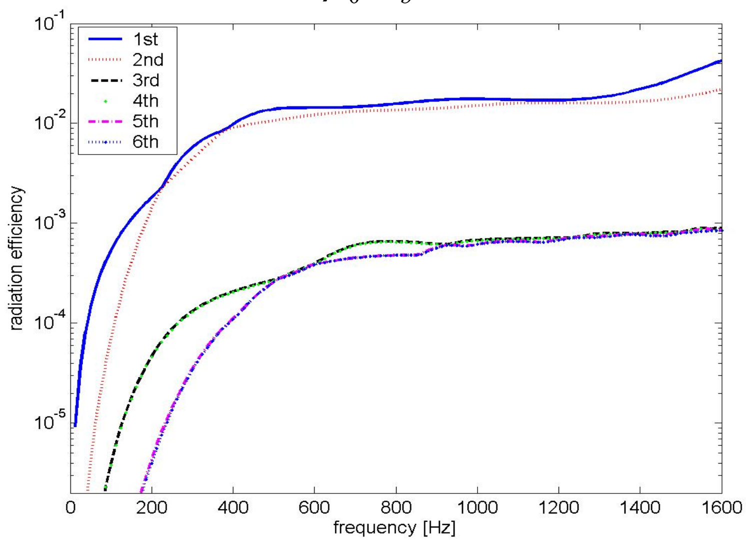

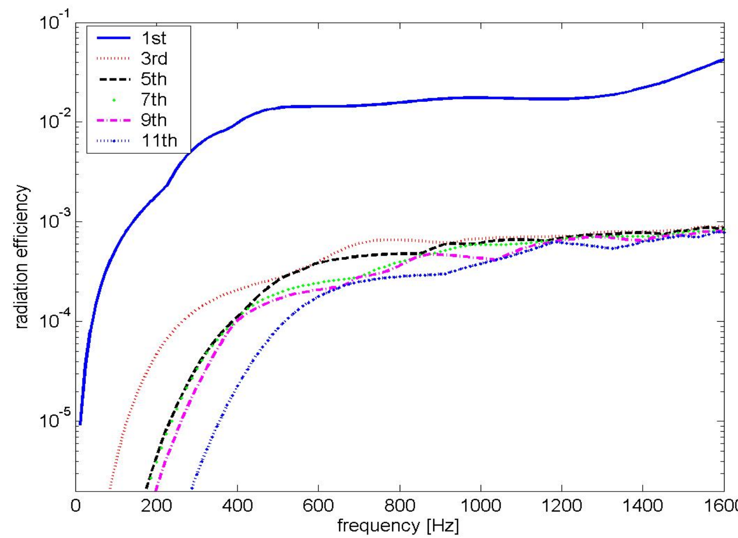

- Radiation modes in same group have equal radiation efficiencies.
- Radiation efficiencies of 1st and 2nd modes are higher than other modes.
- As frequency increases, radiation efficiency of each radiation mode increases.
  Radiation efficiency stops increasing and converges at the coincidence frequency.

Radiation Efficiency of Radiation Modes

[reflecting surface radiation]

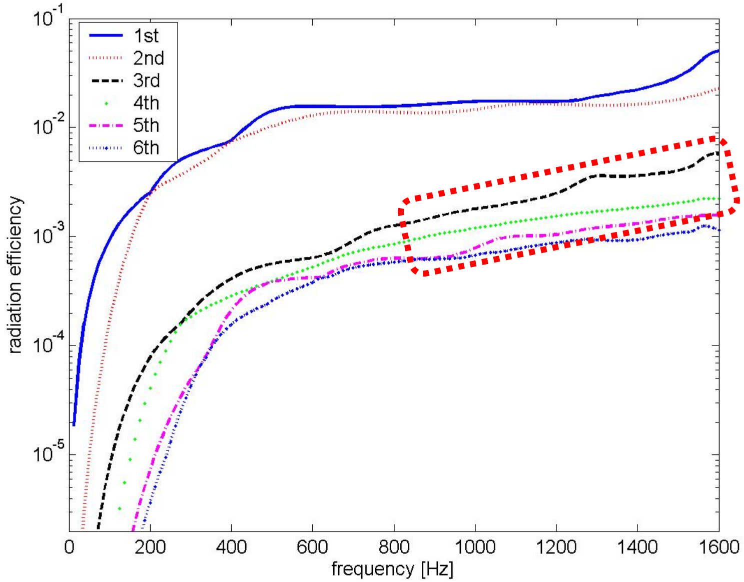

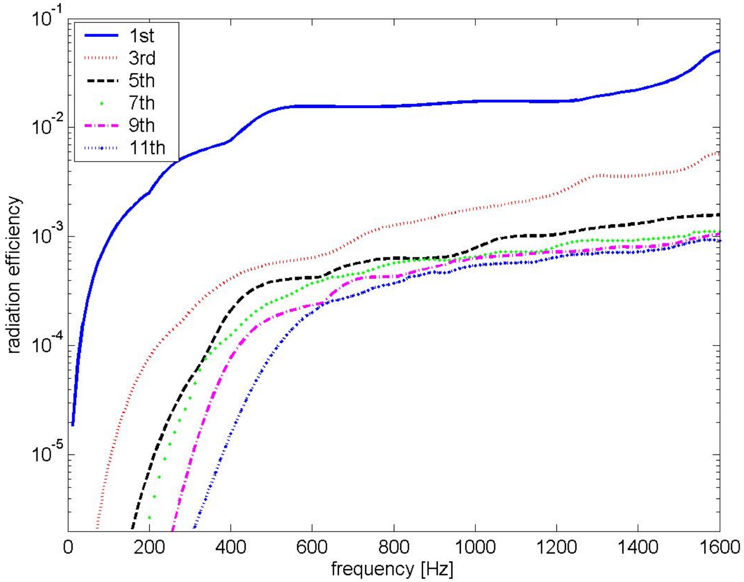

- Grouping characteristic does not appear.
- Radiation efficiencies of 1st and 2nd modes are higher than other modes.
- **Big difference from the free space radiation**
  - Radiation efficiencies of 3rd, 4th and 5th modes increases above 800Hz.

strong radiation region from the contact patch area: Horn Effect

Structural FE Analysis

■ Tire FE model

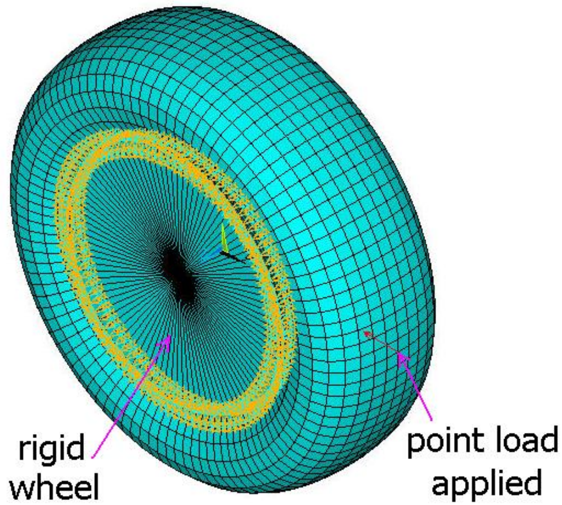

- Shell elements were used.
- To consider stiff belt and rubberized carcass, **orthotropic material properties** were applied on treadband and sidewall.
- Wheel and boundary between wheel and tire were modeled as rigid.
- inflation pressure: 30 psi

■ Structural Harmonic Analysis

- Full matrix method was performed using ANSYS ver. 7.1.
- Harmonic point source was applied at the point in contact with the ground.
- Frequency range: 12.5 Hz – 1600 Hz (constant bandwidth 12.5 Hz)

Orthotropic Material Properties

tread band	circumferential Young's modulus	750 MPa	side wall	circumferential Young's modulus	7.5 MPa
	cross-sectional Young's modulus	320 MPa		cross-sectional Young's modulus	50 MPa
	shear modulus	50 MPa		shear modulus	1.5 MPa
	Possion's ratio	0.45		Possion's ratio	0.45
	density	1200 kg/m^3		density	800 kg/m^3
inflation pressure		30 psi (207 kPa)			

- adapted from the work of Kropp [1989] and Pinnington and Briscoe [2002] or based on physical reasoning, or obtained by direct measurement at Continental Tire.

Structural Wave Propagation

■ Circumferential Wave Number Decomposition

structural velocity distribution in space domain

structural velocity distribution in wave number domain

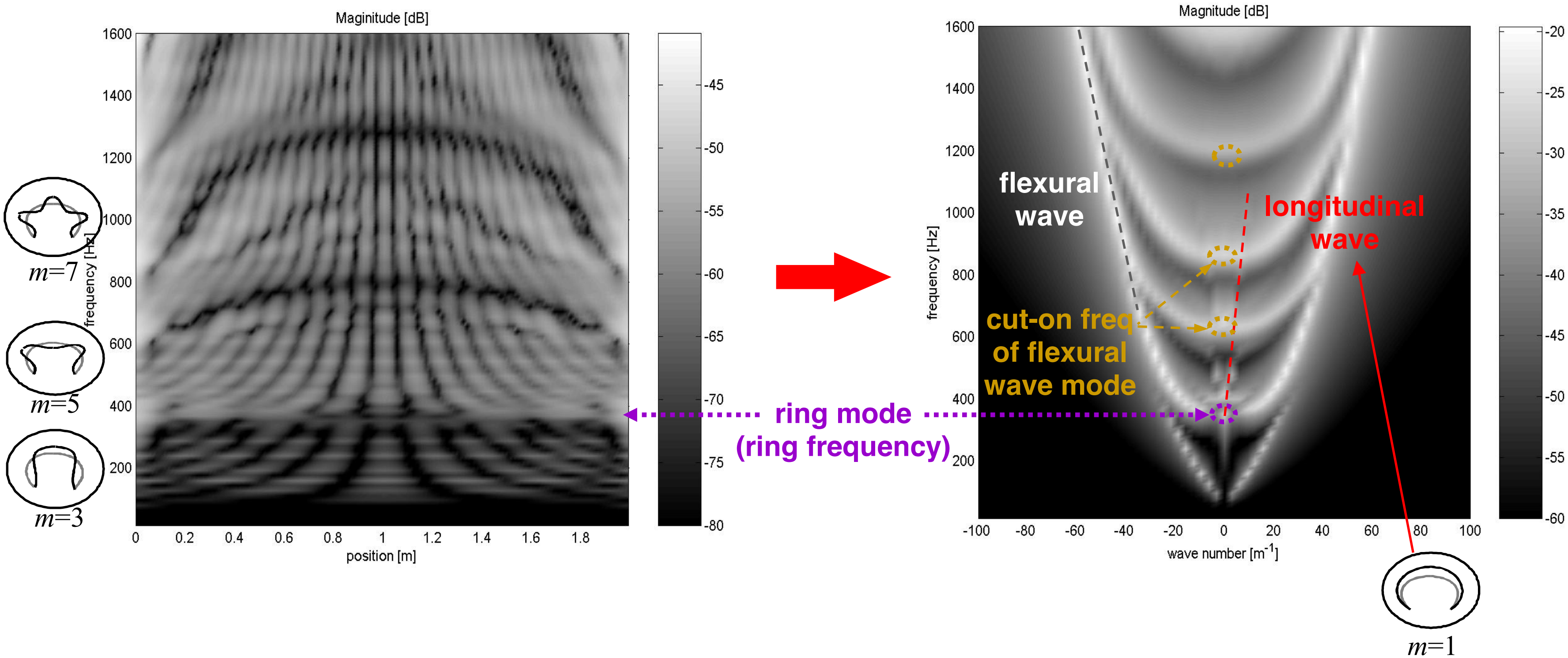

Power Calculation

■ **Structural input power**

proportional to space-averaged mean square velocity.

$$E = \rho_0 c S_b \left\langle \overline{v}_b^2 \right\rangle$$

where S_b: tire surface area

■ **Radiated sound power**

calculated at field points on the recovery surface by using D-BEM directly.

$$W = \sum_{r=1}^{R} \mathrm{Re}[p_r v_r] S_r$$

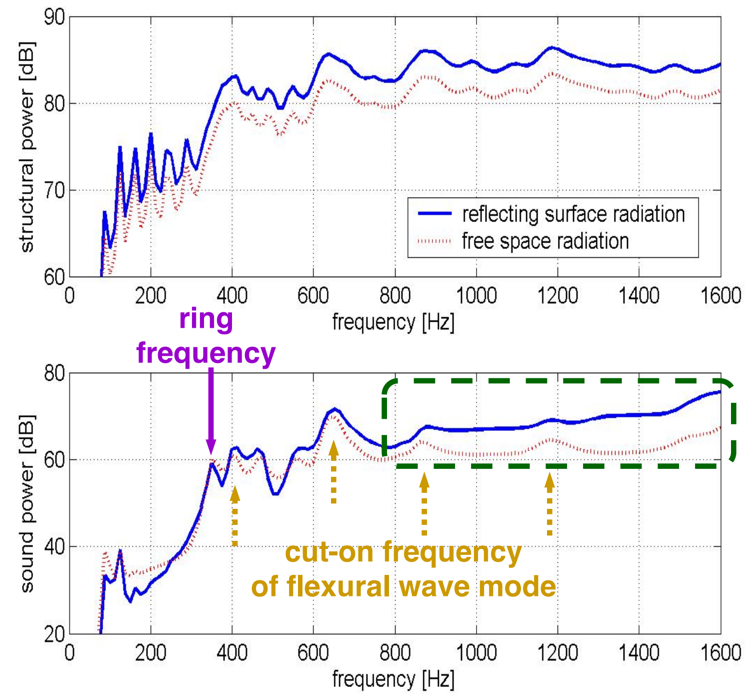

■ **Sound Radiation Characteristics**

– Strong contribution to sound radiation results from the structural waves with low wave number.

– Sound amplification appear above 800 Hz: **Horn Effect**

Matching of Radiation Modes

■ Matching of radiation mode and structural velocity distribution: $|y_n|$

$$W = \mathbf{v}_b^{\mathrm{H}} \mathbf{Q} \boldsymbol{\Lambda} \mathbf{Q}^{\mathrm{H}} \mathbf{v}_b = \mathbf{y}^{\mathrm{H}} \boldsymbol{\Lambda} \mathbf{y} = \sum_{n=1}^{N} W_n = \sum_{n=1}^{N} \lambda_n |y_n|^2$$

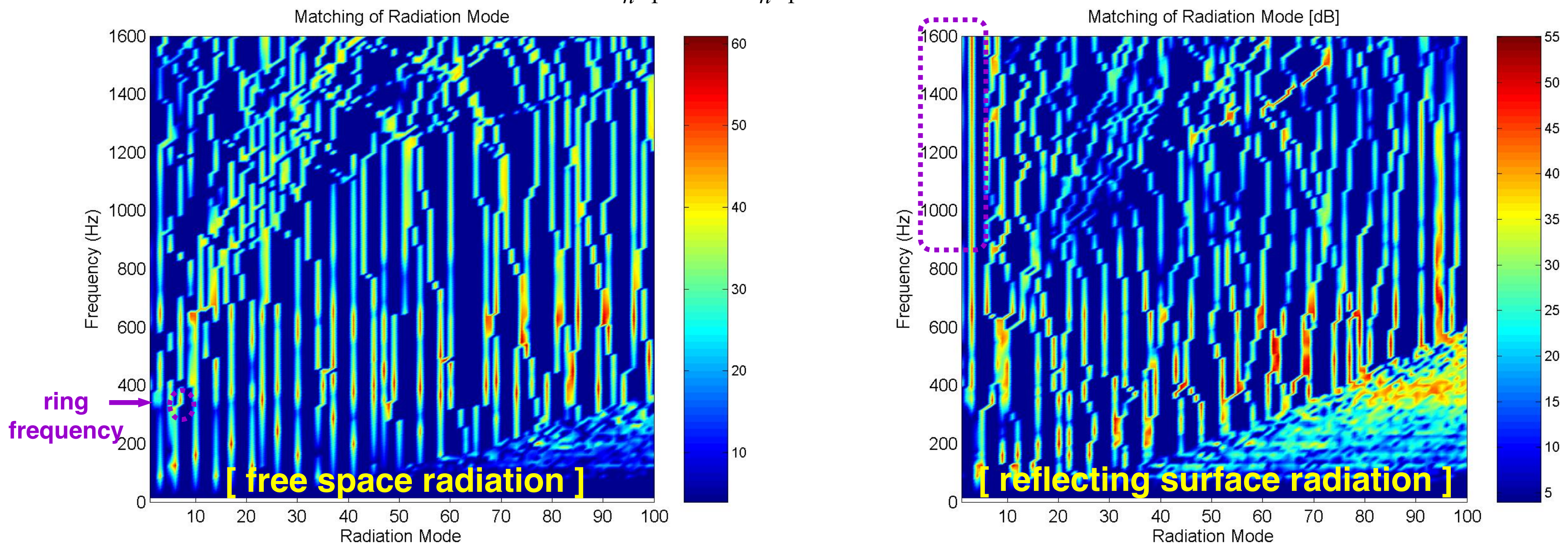

- It shows the relationship between radiation modes and structural velocity on tire surface.
- **All radiation modes do not match with structural velocities**.
- The radiation mode which has a nodal line on the center circumference or on the cross-section including the point in contact with the ground can be neglected.

Sound Power Contribution of Radiation Modes

■ Sound power contribution of each radiation mode when combined with structural velocities

$$W = \mathbf{y}^{\mathrm{H}}\mathbf{\Lambda}\mathbf{y} = \sum_{n=1}^{N} \lambda_n \left| y_n \right|^2 = \sum_{n=1}^{N} \underline{W_n}$$

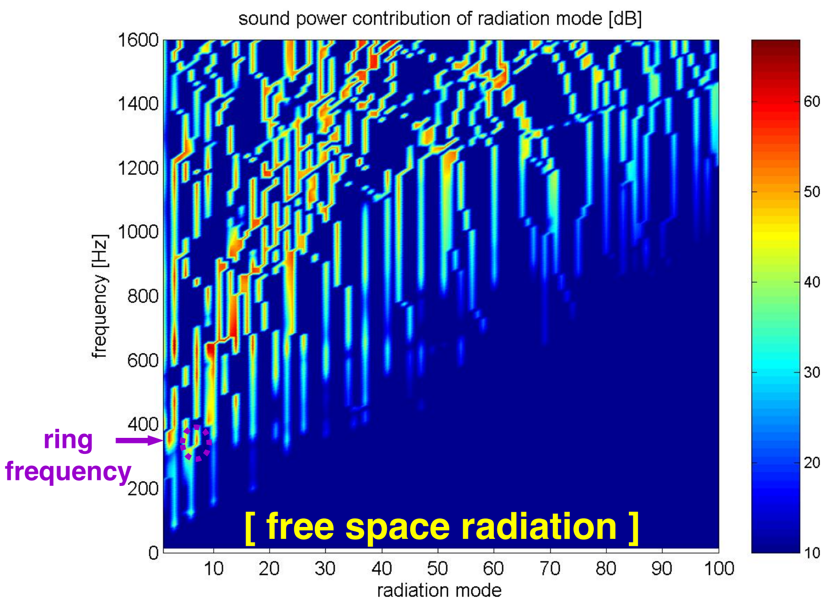

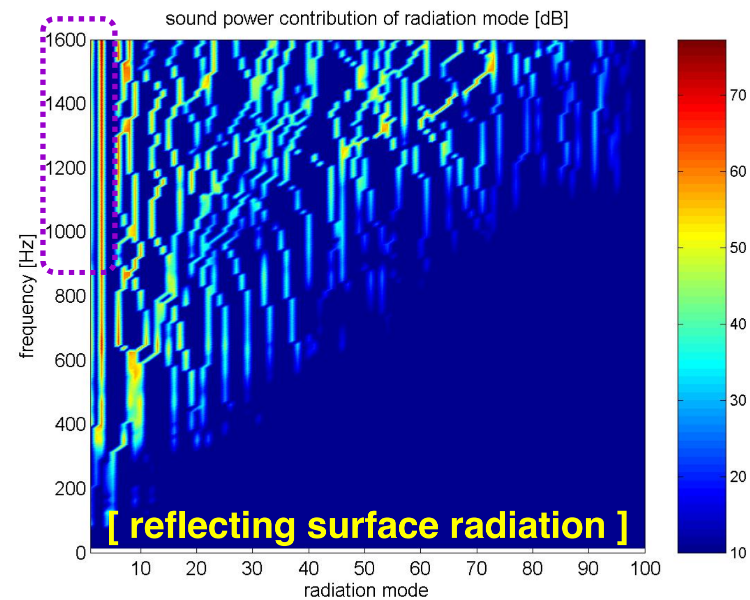

- **All radiation modes do not contribute to the sound radiation.**
- Reflecting surface radiation: **3rd mode is dominant above 800 Hz (Horn Effect Characteristic)**

Cumulative Sound Power Curve

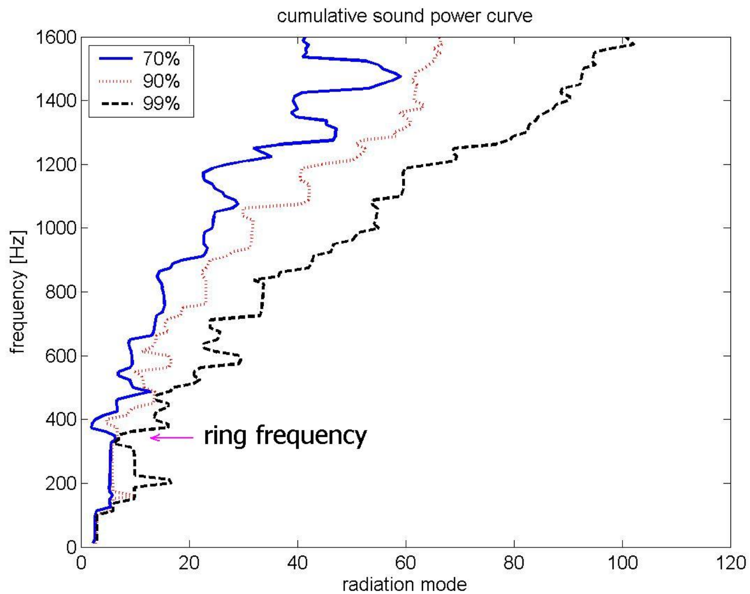

[free space radiation]

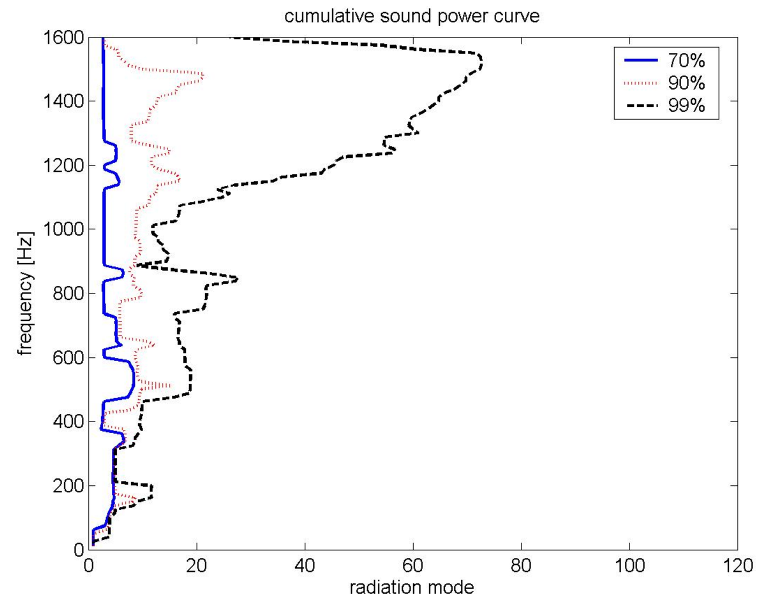

[reflecting surface radiation]

- Free space radiation: 7th radiation mode, a ring-like mode on the treadband, contributes more than 90 percent of the radiated power at the **ring frequency**.
- Reflecting surface radiation: 3rd mode’s contribution is over 70 % above 800 Hz.

Radiated Sound Power

■ Sound Power Calculation

- direct calculation: $W = \sum_{r=1}^{R} \mathrm{Re}[p_r v_r] S_r$
- radiation mode summation: $W = \mathbf{v}_b^{\mathbf{H}} \mathbf{Q} \mathbf{\Lambda} \mathbf{Q}^{\mathbf{H}} \mathbf{v}_b = \mathbf{y}^{\mathbf{H}} \mathbf{\Lambda} \mathbf{y} = \sum_{n=1}^{N} W_n = \sum_{n=1}^{N} \lambda_n |y_n|^2$

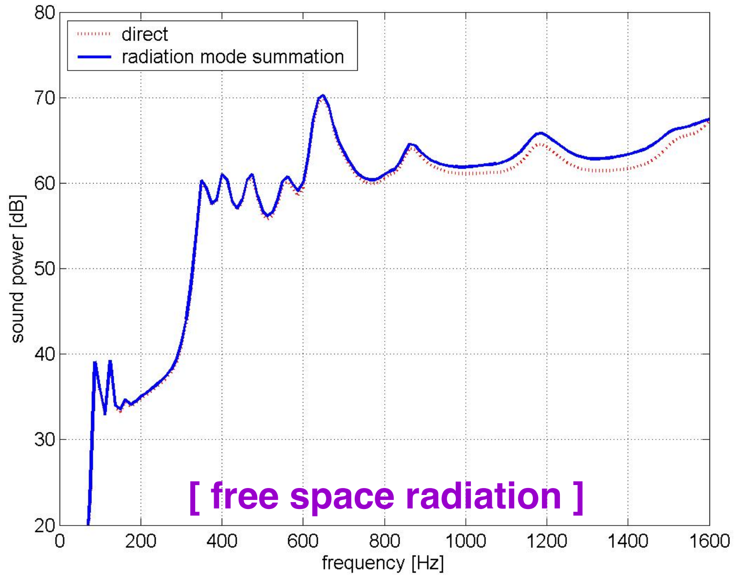

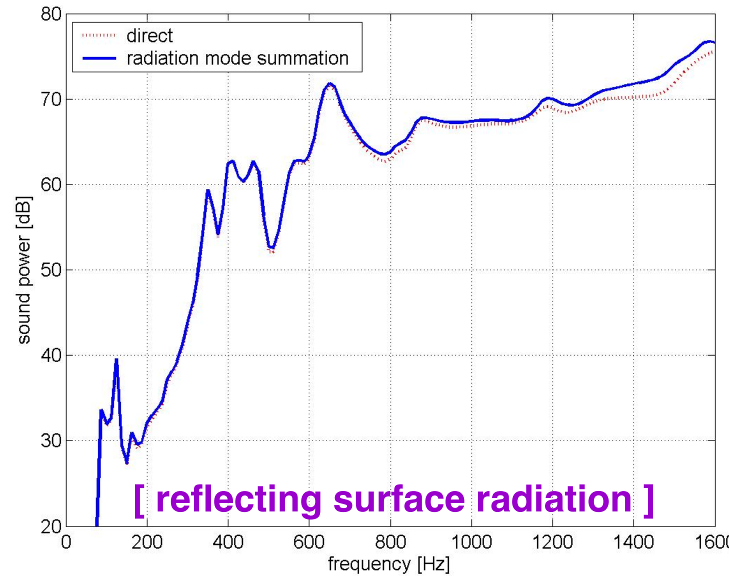

- Good match below 1 kHz between direct calculation and radiation mode summation.
- Radiation mode summation method can be used in sound power calculation.
- If the radiation modes are known, it can reduce the time to calculate the sound power.

Conclusions

- Radiation mode approach for the rectangular plate model and the tire model was implemented by using Acoustic Transfer Function (ATV) in SYSNOISE.
- Radiation mode approach can help us to identify the radiated noise generation mechanism.
- Specifically, the **radiation characteristics** of a three-dimensional tire model in contact with a reflecting surface and enclosed by a hemispherical recovery surface was estimated by using acoustic radiation modes and by comparison with free-space radiation.
- The third radiation mode above 800 Hz is principally responsible for the **horn effect** in the presence of reflecting surface.
- The significance of the **fast, longitudinal wave** mode propagating through the treadband was confirmed by the large contribution of the modified ring radiation mode to the radiated sound power at the tire’s ring frequency.

References

1. K. Yum and J. S. Bolton, 2004, "Sound Radiation Modes of a Tire on a Reflecting Surface," *Proc NOISE-CON 2004*, pp. 161-168.
2. S. J. Elliot and M. E. Johnson, 1993, "Radiation Modes and the Active Control of Sound Power," *J. Acoust. Soc. Am.* Vol. 94(4), pp. 2194-2204.
3. K. A. Cunefare and M. N. Currey, 1994, "On the Exterior Acoustic Modes of Structures," *J. Acoust. Soc. Am.* Vol. 96(4), pp. 2302-2312.
4. K. A. Cunefare, M. N. Currey, M. E. Johnson and S. J. Elliot, 2001, "The Radiation Efficiency Grouping of Free-Space Acoustic Radiation Modes," *J. Acoust. Soc. Am*. Vol. 109(1), pp. 203-215.
5. M. Tournour, P. Brux, et al., 2003, "Inverse Numerical Acoustics of a Truck Engine," *SAE Paper 2003-01-1692.*
6. F. Martinus, D. W. Herrin and A. F. Seybert, "Practical Considerations in Reconstructing the Surface Vibration using Inverse Numerical Acoustics," *SAE Paper 03NVC-113*.
7. 2000, *SYSNOISE Rev 5.5: User Manual*, LMS International.
8. H. A. Schenck, 1968, "Improved Integral Formulation for Acoustic Radiation Problems," *J. Acoust. Soc. Am.* Vol. 44(1), pp. 41-58.